Journal of Zhejiang University-SCIENCE C (Computers & Electronics)
ISSN 1869-1951 (Print); ISSN 1869-196X (Online)
www.zju.edu.cn/jzus; www.springerlink.com
E-mail: jzus@zju.edu.cn

Examination of the wavelet-based approach for measuring self-similarity of epileptic electroencephalogram data

Suparerk JANJARASJITT
(*Department of Electrical and Electronic Engineering, Ubon Ratchathani University, Ubon Ratchathani 34190, Thailand*)
E-mail: suparerk.j@ubu.ac.th

Received Apr. 5, 2014; Revision accepted July 18, 2014; Crosschecked Nov. 18, 2014

Abstract: Self-similarity or scale-invariance is a fascinating characteristic found in various signals including electroencephalogram (EEG) signals. A common measure used for characterizing self-similarity or scale-invariance is the spectral exponent. In this study, a computational method for estimating the spectral exponent based on wavelet transform was examined. A series of Daubechies wavelet bases with various numbers of vanishing moments were applied to analyze the self-similar characteristics of intracranial EEG data corresponding to different pathological states of the brain, i.e., ictal and interictal states, in patients with epilepsy. The computational results show that the spectral exponents of intracranial EEG signals obtained during epileptic seizure activity tend to be higher than those obtained during non-seizure periods. This suggests that the intracranial EEG signals obtained during epileptic seizure activity tend to be more self-similar than those obtained during non-seizure periods. The computational results obtained using the wavelet-based approach were validated by comparison with results obtained using the power spectrum method.

Key words: Self-similarity, Power-law behavior, Wavelet analysis, Electroencephalogram, Epilepsy, Seizure
doi:10.1631/jzus.C1400126 **Document code:** A **CLC number:** TN911.7; R318

1 Introduction

Concepts and computational methods derived from the contemporary study of complex systems, including chaos theory, nonlinear dynamics, and fractals, have gained increasing interest for applications in biology and medicine because physiological signals and systems can exhibit an extraordinary range of patterns and behaviors (Goldberger, 2006). The mathematical concept of a fractal is commonly associated with irregular objects that exhibit a property called self-similarity of scale-invariance (Mandelbrot, 1982; Goldberger, 2006). Fractal forms are composed of subunits resembling the structure of the macroscopic object (Goldberger, 2006) which in nature can emerge from statistical scaling behavior in the underlying physical phenomena (Wornell, 1995). Further, many physical, biological, or physiological signals may exhibit not just a simple monofractal scaling behavior (Kantelhardt *et al.*, 2002). Multifractal signals are associated with different self-similar behaviors on various scales ranging from small to large. Multifractal geometry has been extensively applied to many biomedical signal analysis applications (Lopes and Betrouni, 2009).

An important class of statistical scale-invariant or self-similar random processes is the $1/f$ processes (Wornell, 1995). A traditional mathematical model and the empirical properties of $1/f$ processes have been inspired largely by the fractional Brownian motion framework (Wornell and Oppenheim, 1992; Wornell, 1993; 1995) as developed by Mandelbrot and van Ness (1968). In general, models of $1/f$ processes are represented using a frequency domain characterization. The dynamics of $1/f$ processes exhibit power law behavior (Watters, 1998)

ORCID: Suparerk JANJARASJITT, http://orcid.org/0000-0002-0252-8795

and can be characterized in the frequency domain by $S(\omega) \propto 1/|\omega|^{\gamma}$, where $S(\omega)$ is the Fourier transform and γ is referred to as the spectral exponent. Accordingly, the spectral exponent γ can be inherently obtained from the slope of a log-log plot of power spectral density.

Flicker-noise spectroscopy (FNS) is another method relevant to the concept of $1/f$ processes. The main idea of FNS is that the power spectrum of many natural signals has a plateau at lower frequencies, but flicker noise at higher frequencies (Timashev and Polyakov, 2007; Timashev *et al.*, 2010). Such behavior results in a finite correlation scale for the $1/f$ noise component (Timashev and Polyakov, 2007; Timashev *et al.*, 2010). The FNS method has been applied to various biomedical signals, e.g., electroencephalogram (EEG) (Timashev *et al.*, 2012) and magnetoencephalogram (MEG) (Timashev *et al.*, 2009). Wornell (1993; 1995) developed a wavelet-based representation for $1/f$ processes. As the wavelet transform is a natural tool for characterizing self-similar or scale-invariant signals, wavelet transformations play a significant role in the study of self-similar signals and systems (Wornell, 1995).

In this study, a computational method based on a wavelet-based representation of $1/f$ processes developed by Wornell (1991) is used to estimate the spectral exponent which characterizes the self-similarity of a signal. The wavelet-based approach was shown to provide better performance compared to detrended fluctuation analysis (DFA) (Janjarasjitt, 2014). Furthermore, the wavelet-based approach was previously applied to examine the self-similarity or the scale-invariant characteristics of long-term continuous electrocorticogram (ECoG) data recorded from epilepsy patients (Janjarasjitt and Loparo, 2009; 2010). They showed that the epileptic ECoG data corresponding to various pathological and physiological states of the brain exhibit distinctive scale-invariant characteristics.

In this study, a series of Daubechies wavelet bases corresponding to various numbers of vanishing moments was evaluated. The application of the wavelet-based approach to epileptic EEG data analysis is demonstrated. The wavelet-based approach was validated by comparison to the conventional method, i.e., the power spectrum method. The sets of epileptic EEG data used in this study have been used in several studies and examined using various computational approaches for epileptic seizure classification and detection. For example, Pachori (2008) and Pachori and Patidar (2014) used empirical mode decomposition (EMD) to extract features of epileptic EEG data for seizure classification while Joshi *et al.* (2014) used the error energy obtained using fractional linear prediction (FLP) as a feature for epileptic seizure detection. The computational results showed that these approaches can provide a high classification rate.

2 Methods

2.1 $1/f$ processes

In general, models of $1/f$ processes are represented using a frequency domain characterization. The dynamics of $1/f$ processes exhibit power-law behavior (Watters, 1998) and can be characterized in the form of (Wornell, 1993; 1995)

$$S_x(\omega) \sim \frac{\sigma_x^2}{|\omega|^{\gamma}} \tag{1}$$

over several decades of frequency ω with a variance of σ_x^2. The spectral exponent γ thus specifies a distribution of spectral content from low to high frequencies. An increase in γ leads to a sample function with smoother temporal patterns (Wornell, 1993; 1995).

2.2 Wavelet-based representation of $1/f$ processes

The following theorem introduces the wavelet-based representation for $1/f$ processes:

Theorem 1 (Wornell, 1993) The random process $x(t)$ can be constituted by wavelet basis expansions

$$x(t) = \sum_m \sum_n d_{m,n} \psi_{m,n}(t), \tag{2}$$

where $\psi_{m,n}(t)$ is an orthonormal wavelet basis with Rth-order regularity, m and n are respectively, the dilation and translation indices, and $d_{m,n}$ are the wavelet coefficients, a collection of mutually uncorrelated, zero-mean random variables, with the geometric scale-to-scale variance progression

$$\mathrm{var}(d_{m,n}) = \sigma^2 2^{-\gamma m} \tag{3}$$

for some parameter γ $(0 < \gamma < 2R)$. The time-average spectrum of the process $x(t)$ is given by

$$S_x(\omega) = \sigma^2 \sum_m 2^{-\gamma m} |\Psi\left(2^{-m}\omega\right)|^2, \tag{4}$$

which is nearly $1/f$, i.e.,

$$\frac{\sigma_{\mathrm{L}}^2}{|\omega|^\gamma} \le S_x(\omega) \le \frac{\sigma_{\mathrm{U}}^2}{|\omega|^\gamma} \tag{5}$$

for some $0 < \sigma_{\mathrm{L}}^2 \le \sigma_{\mathrm{U}}^2 < \infty$ where σ_{L}^2 and σ_{U}^2 are bounding constants, and has exponentially spaced ripple such that

$$|\omega|^\gamma S_x(\omega) = |2^k\omega|^\gamma S_x\left(2^k\omega\right),\ \forall\ k \in \mathbb{Z}. \tag{6}$$

The spectral exponent γ of a $1/f$ process is directly related to the self-similarity parameter H (Wornell and Oppenheim, 1992; Wornell, 1993; 1995). This is also indicative of long-range correlations (Goldberger *et al.*, 2002).

2.3 Wavelet-based self-similarity measure

According to Theorem 1, the spectral exponent γ of a $1/f$ process can be determined from a linear relationship between $\log_2 \mathrm{var}(d_{m,n})$ and the level m. Therefore, the wavelet-based approach for estimating the spectral exponent can be performed in the following steps:

1. Normalize a signal $\{x[n]\}$ for $n = 0, 1, \ldots, N-1$ by factoring with its norm which is $x_{\mathrm{n}}[n] = x[n]/\sum_k x^2[k]$.

2. Decompose the normalized signal $\{x_{\mathrm{n}}[n]\}$ into M levels using the wavelet-basis expansions to obtain the wavelet coefficients $d_{m,n}$, where $m = 1, 2, \ldots, M$.

3. Compute the variance of wavelet coefficients $d_{m,n}$ corresponding to each level m.

4. Compute the logarithm to base 2 of the corresponding variances of wavelet coefficients $\mathrm{var}(d_{m,n})$.

5. Estimate the slope of the $\log_2 \mathrm{var}(d_{m,n})$-$m$ plot to obtain γ.

3 Data and analysis

3.1 Data and patients

The data examined in this study consist of two sets of intracranial EEG data of epilepsy patients obtained from the Department of Epileptology, University of Bonn (http://epileptologie-bonn.de/cms/front_content.php?idcat=193) and originated from Andrzejak *et al.* (2001). The intracranial EEG data sets, referred to as N and S, were recorded using intracranial electrodes from five epilepsy patients whom had achieved complete seizure control after resection of one of the hippocampal formations (Andrzejak *et al.*, 2001). The data set N corresponds to intracranial EEG signals during non-seizure periods (interictal state), while the data set S was recorded during seizure activity (ictal state). Both data sets were recorded from within the epileptogenic zone (Andrzejak *et al.*, 2001).

Each intracranial EEG data set contains 100 epochs of a single-channel intracranial EEG signal recorded with a 128-channel amplifier system using an average common reference (omitting electrodes containing pathological activity) (Andrzejak *et al.*, 2001). The length of each epoch is 4096 samples (about 23.6 s). These epochs were selected and cut out from continuous multi-channel intracranial EEG data recordings after visual inspection for artifacts, including muscle activity and eye movements (Andrzejak *et al.*, 2001). In addition, the epochs of the intracranial EEG signal satisfied the weak stationarity criterion given in Andrzejak *et al.* (2001). The intracranial EEG data were sampled with 12-bit analog-to-digital conversion and a sampling rate of 173.61 Hz. The intracranial EEG data had a spectral bandwidth of between 0.5 and 85 Hz. Examples of the signals for each data set are depicted in Fig. 1.

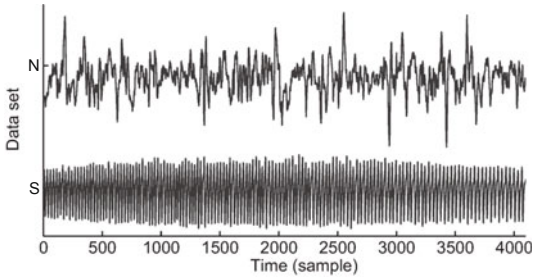

Fig. 1 Example of the intracranial EEG signals of data sets N and S

3.2 Analytic framework

In the computational analysis, the intracranial EEG signals were decomposed into four levels, i.e., m = 1, 2, 3, and 4, using a family of Daubechies wavelet bases. Four types of Daubechies wavelet bases were examined, including the 1st order (referred to as Db1) and also known as Haar wavelets, the 2nd order (Db2), the 10th order (Db10), and the 30th order (Db30). All these types of Daubechies wavelet bases are orthogonal and have compact

supports. The number of vanishing moments of the Daubechies wavelet bases varied. The higher the order, the higher the number of vanishing moments.

The corresponding spectral sub-bands of the wavelets at levels $m = 1$, 2, 3, and 4 approximately fail in the ranges of $\geq$ 43.40 Hz, 21.70–43.40 Hz, 10.85–21.70 Hz, and 5.43–10.85 Hz, respectively. The spectral sub-bands of the 10th order of Daubechies wavelets corresponding to levels $m = 1$, 2, 3, and 4 are illustrated in Fig. 2. The spectral exponent was estimated using the $\log_2$-var of wavelet coefficients corresponding to only the levels $m = 1$, 2, and 3, as the linear relationship between the $\log_2$-var of wavelet coefficients of the intracranial EEG signals is practically observed. The slope of the $\log_2$-var of wavelet coefficients was estimated using the least squares estimator.

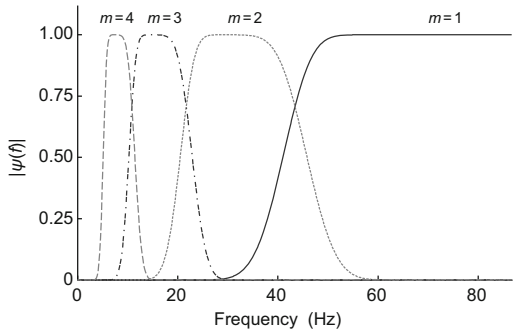

Fig. 2 The corresponding spectral sub-bands of the 30th order of Daubechies wavelets at the levels m=1, 2, 3, and 4

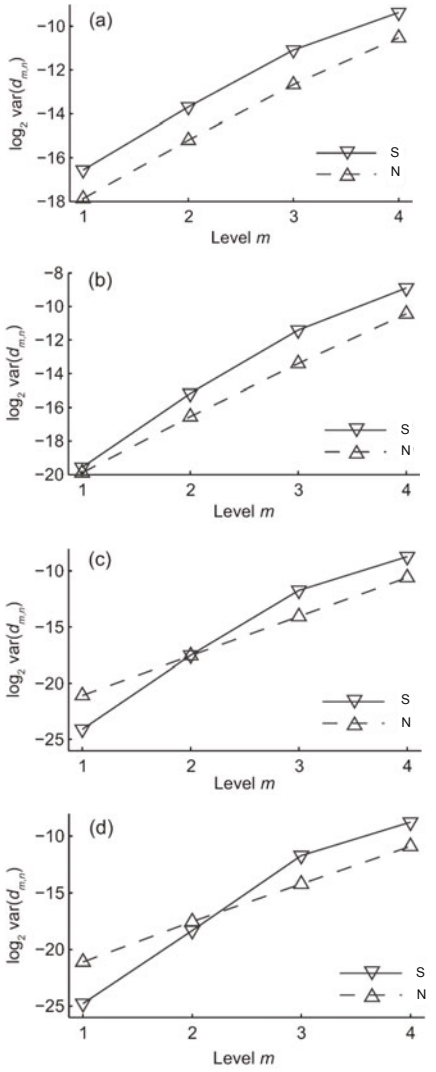

Fig. 3 Comparison of $\log_2$-var of wavelet coefficients of the exemplary intracranial EEG signals of data sets N and S using Daubechies wavelet bases Db1 (a), Db2 (b), Db10 (c), and Db30 (d)

4 Results

4.1 Characteristics of the spectral exponents

Plots of the $\log_2$-var of wavelet coefficients of the exemplary intracranial EEG signals of data sets N and S are shown in Fig. 1 and those using different Daubechies wavelet bases are illustrated in Fig. 3. The $\log_2$-var of wavelet coefficients of the signals varied corresponding to the wavelet bases but showed the power-law behavior. The estimated spectral exponents of the exemplary intracranial EEG signal of data set N obtained using the Db1, Db2, Db10, and Db30 wavelets were 2.6007, 3.2422, 3.5030, and 3.4412, respectively, while those of data set S obtained using the Db1, Db2, Db10, and Db30 wavelet bases were 2.7380, 4.0782, 6.1793, and 6.5373, respectively.

Table 1 summarizes the statistical values of the $\log_2$-var of wavelet coefficients of all intracranial EEG data of both sets using the Db1, Db2, Db10, and Db30 wavelet bases. At the same level of m, the $\log_2$-var of wavelet coefficients tended to decrease as the order of Daubechies wavelet bases increased. In particular, at the level $m = 1$ or $m = 2$, the $\log_2$-var of wavelet coefficients of all intracranial EEG data using the Db10 and Db30 wavelet bases were substantially lower than those using the Db1 and Db2 wavelet bases. In addition, the $\log_2$-var of

wavelet coefficients of the data set S tended to be affected more by the order of Daubechies wavelet bases. This could be because the number of vanishing moments of the Daubechies wavelet bases increases as the order of Daubechies wavelet bases increases. The higher order of the Daubechies wavelet bases (those with a higher number of vanishing moments) can better represent the higher frequency components of the intracranial EEG signals.

The estimated spectral exponents of the intracranial EEG data sets N and S obtained using the Db1, Db2, Db10, and Db30 wavelet bases are compared in box plots shown in Fig. 4. Also, the statistical values of the spectral exponents are summarized in Table 2. The estimated spectral exponent tended to increase as the order of Daubechies wavelet bases used increased. The estimated spectral exponents of the intracranial EEG data sets N and S obtained using the Db1 wavelet bases were generally comparable, while those obtained using the Db2, Db10, or Db30 wavelet bases were substantially different. Furthermore, the estimated spectral exponents of the data set S typically tended to be higher than those of set N.

Table 1 The statistical values of the $\log_2$-var of wavelet coefficients of the intracranial EEG data sets N and S

Wavelet bases	Level m	$\log_2$ var N	$\log_2$ var S
Db1	1	−17.4643±0.6801	−16.2591±0.6413
	2	−14.8262±0.6051	−13.5173±0.6117
	3	−12.4121±0.5550	−11.2634±0.5204
	4	−10.5041±0.5301	−9.9491 ± 0.5676
Db2	1	−19.3189±1.0183	−18.4120±0.9401
	2	−15.9483±0.8019	−14.3411±0.8532
	3	−12.8670±0.6794	−11.3788±0.6512
	4	−10.5244±0.6266	−9.8392 ± 0.7422
Db10	1	−20.6040±1.4719	−21.8310±1.3752
	2	−16.9059±1.0470	−15.5034±1.1135
	3	−13.3456±0.7467	−11.4474±0.8220
	4	−10.6035±0.7781	−9.8489 ± 0.9126
Db30	1	−20.7005±1.5331	−22.3388±1.4176
	2	−17.0008±1.1097	−15.7466±1.1698
	3	−13.4762±0.7417	−11.4414±0.8457
	4	−10.6492±0.7633	−9.8839 ± 0.9320

Statistical values are expressed as mean±standard deviation

4.2 Validation of the wavelet-based approach

To validate the estimated spectral exponents obtained using the wavelet-based approach, the spectral exponents of the intracranial EEG data were computed from the power spectrum estimated using the Yule-Walker AR method with the order of four. Plots of the power spectral density of the exemplary intracranial EEG signals of data sets N and S are shown in Fig. 5. These reveal that the signals exhibit power-law behavior. In addition, there is a change in the slope of the power spectral density of the exemplary intracranial EEG signals at around 10 Hz, which is similar to the $\log_2$-var of wavelet coefficients whose slope changes at level of three.

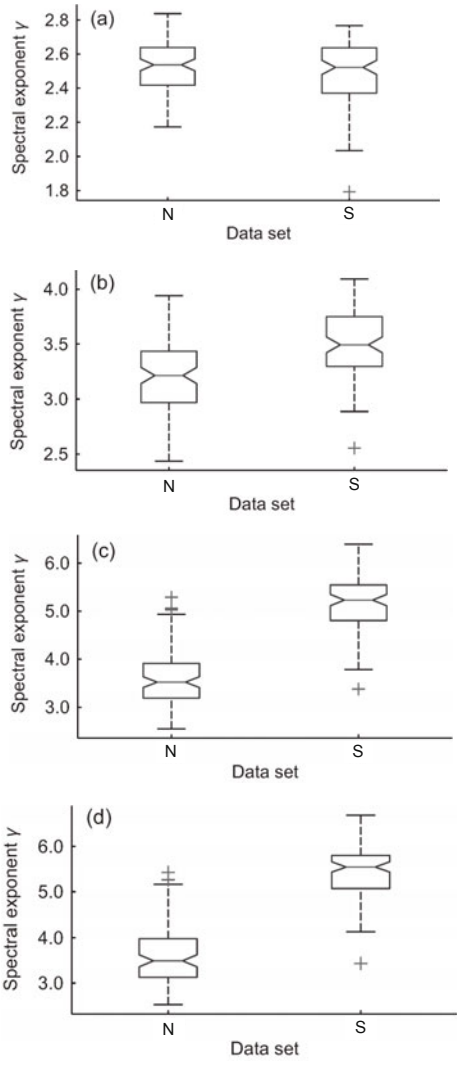

Fig. 4 Comparison of the spectral exponents of the intracranial EEG data sets N and S using Daubechies wavelet bases Db1 (a), Db2 (b), Db10 (c), and Db30 (d)

The spectral exponents of the exemplary intracranial EEG signals of data sets N and S (Fig. 1) estimated from the frequency ranges $\geq$ 10.85 Hz and

Table 2 The statistical values of the spectral exponents of the intracranial EEG data of sets N and S

Wavelet bases	$\log_2$ var	
	N	S
Db1	2.5261 ± 0.1396	2.4979 ± 0.1767
Db2	3.2260 ± 0.3125	3.5166 ± 0.3122
Db10	3.6292 ± 0.6003	5.1918 ± 0.5559
Db30	3.6121 ± 0.6667	5.4487 ± 0.5886

Statistical values are expressed as mean±standard deviation

higher using the power spectrum method were 3.0514 and 5.3451, respectively. As observed previously, the estimated spectral exponent of the EEG signal of data set S was higher than that of data set N.

The estimated spectral exponents of the intracranial EEG data sets N and S obtained using the power spectrum method are compared using box plots shown in Fig. 6. The spectral exponents estimated using the power spectrum method are equivalent to those estimated using the wavelet-based approach, especially with the Db10 and Db30 wavelet bases. In addition, the statistical values of the spectral exponents obtained using the power spectrum method were, respectively, 3.1769 ± 0.5541 and 4.8241 ± 0.5155. This supports the finding that the spectral exponents of the intracranial EEG data of set S tend to be higher than those of set N. Furthermore, the estimated spectral exponents of the EEG data obtained using the power spectrum method were similar to those obtained using the wavelet-based approach.

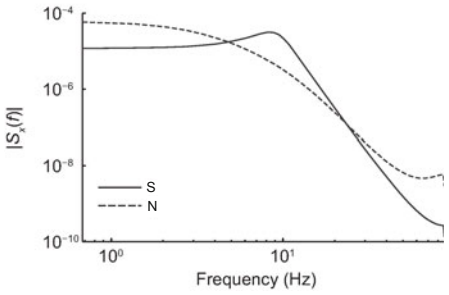

Fig. 5 Comparison of the power spectral density of the exemplary intracranial EEG signals of data sets N and S using the Yule-Walker AR method

5 Discussion and conclusions

Our results show that an approach based on a wavelet-based representation of $1/f$ processes (Wornell, 1993) can be used successfully to estimate the spectral exponent γ, which characterizes self-similarity. The spectral exponents of the intracranial EEG signals estimated using the wavelet-based approach were generally comparable to those estimated using the power spectrum method. In particular, the interpretations of the computational results obtained from both methods are identical. However, the wavelet transform method is naturally suited for manipulating self-similar or scale-invariant signals, while the Fourier transform method is suited for translation-invariant signals such as stationary, cyclostationary, and periodic signals (Wornell, 1991). Moreover, the implementation of wavelet transformations using fast discrete wavelet transform makes the wavelet-based approach more practical. Abry *et al.* (1993) showed that the wavelet-based approach can be used to estimate the power spectral density. As a result, the wavelet-based approach can increase the accuracy of the estimation of the spectral exponent.

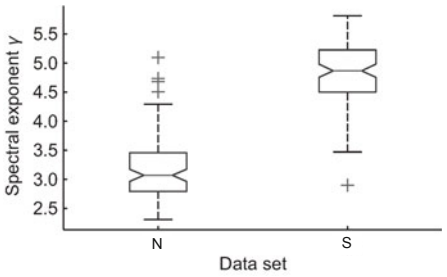

Fig. 6 Comparison of the spectral exponents of the intracranial EEG data of sets N and S using the power spectrum method

From the application viewpoint, the computational results suggest that intracranial EEG signals obtained during epileptic seizure activity tend to be more self-similar than those obtained during non-seizure periods. Even though the estimated spectral exponent was varied and affected by the wavelet bases (in particular, the number of vanishing moments) used in the wavelet-based approach, a significant difference between the spectral exponents obtained during epileptic seizure activity and those obtained during non-seizure periods can be generally observed. This is sufficient to reveal the characteristics of the underlying neuronal dynamics of the brain corresponding to different pathological states, i.e., epileptic seizure activity (ictal state) and

non-seizure period (interictal state). Wavelet bases with sufficiently high numbers of vanishing moments yield consistent spectral exponents. Furthermore, the distinct self-similar characteristics of the intracranial EEG signals may be used for epileptic seizure classification and detection.

The spectral exponents γ of the epileptic EEG data recorded during different states and from different brain regions obtained using the wavelet-based fractal analysis were compared to the correlation dimension (Janjarasjitt and Loparo, 2013) and the Hurst exponent (Janjarasjitt and Loparo, 2014a; 2014b). A similar conclusion was obtained.

References

Abry, P., Goncalves, P., Flandrin, P., 1993. Wavelet-based spectral analysis of $1/f$ processes. IEEE Int. Conf. on Acoustics, Speech, and Signal Processing, p.237-240. [doi:10.1109/ICASSP.1993.319479]

Andrzejak, R.G., Lehnertz, K., Mormann, F., *et al.*, 2001. Indications of nonlinear deterministic and finite-dimensional structures in time series of brain electrical activity: dependence on recording region and brain state. *Phys. Rev. E*, **64**:061907.1-061907.8. [doi:10.1103/PhysRevE.64.061907]

Goldberger, A.L., 2006. Complex systems. *Proc. Am. Thorac. Soc.*, **3**:467-471. [doi:10.1513/pats.200603-028MS]

Goldberger, A.L., Amaral, L.A.N., Hausdorff, J.M., *et al.*, 2002. Fractal dynamics in physiology: alterations with disease and aging. *PNAS*, **99**(suppl 1):2466-2472. [doi:10.1073/pnas.012579499]

Janjarasjitt, S., 2014. Computational validation of fractal characterization by using the wavelet-based fractal analysis. *J. Korean Phys. Soc.*, **64**(6):780-785. [doi:10.3938/jkps.64.780]

Janjarasjitt, S., Loparo, K.A., 2009. Wavelet-based fractal analysis of the epileptic EEG signal. Int. Symp. on Intelligent Signal Processing and Communication Systems, p.127-130. [doi:10.1109/ISPACS.2009.5383886]

Janjarasjitt, S., Loparo, K.A., 2010. Wavelet-based fractal analysis of multi-channel epileptic ECoG. IEEE Region 10 Conf. TENCON, p.373-378. [doi:10.1109/TENCON.2010.5686662]

Janjarasjitt, S., Loparo, K.A., 2013. Comparison of complexity measures using two complex system analysis methods applied to the epileptic ECoG. *J. Korean Phys. Soc.*, **63**(8):1659-1665. [doi:10.3938/jkps.63.1659]

Janjarasjitt, S., Loparo, K.A., 2014a. Examination of scale-invariant characteristics of epileptic electroencephalograms using wavelet-based analysis. *Comput. Electr. Eng.*, **40**(5):1766-1773. [doi:10.1016/j.compeleceng.2014.04.005]

Janjarasjitt, S., Loparo, K.A., 2014b. Scale-invariant behavior of epileptic ECoG. *J. Med. Biol. Eng.*, in press. [doi:10.5405/jmbe.1433]

Joshi, V., Pachori, R.B., Vijesh, A., 2014. Classification of ictal and seizure-free EEG signals using fractional linear prediction. *Biomed. Signal Process. Contr.*, **9**:1-5. [doi:10.1016/j.bspc.2013.08.006]

Kantelhardt, J.W., Zschiegner, S.A., Koscielny-Bunde, E., *et al.*, 2002. Multifractal detrended fluctuation analysis of nonstationary time series. *Phys. A*, **316**(1-4):87-114. [doi:10.1016/S0378-4371(02)01383-3]

Lopes, R., Betrouni, N., 2009. Fractal and multifractal analysis: a review. *Med. Image Anal.*, **13**(4):634-649. [doi:10.1016/j.media.2009.05.003]

Mandelbrot, B.B., 1982. The Fractal Geometry of Nature. W.H. Freeman and Company, San Francisco, USA.

Mandelbrot, B.B., van Ness, J.W., 1968. Fractional Brownian motions, fractional noises and applications. *SIAM Rev.*, **10**(4):422-437. [doi:10.1137/1010093]

Pachori, R.B., 2008. Discrimination between ictal and seizure-free EEG signals using empirical mode decomposition. *Res. Lett. Signal Process.*, **2008**:293056.1-293056.5. [doi:10.1155/2008/293056]

Pachori, R.B., Patidar, S., 2014. Epileptic seizure classification in EEG signals using second-order difference plot of intrinsic mode functions. *Comput. Method. Progr. Biomed.*, **113**(2):494-502. [doi:10.1016/j.cmpb.2013.11.014]

Timashev, S.F., Polyakov, Y.S., 2007. Review of flicker noise spectroscopy in electrochemistry. *Fluct. Noise Lett.*, **7**(2):R15-R47. [doi:10.1142/S0219477507003829]

Timashev, S.F., Polyakov, Y.S., Yulmetyev, R.M., *et al.*, 2009. Analysis of biomedical signals by flicker-noise spectroscopy: identification of photosensitive epilepsy using magnetoencephalograms. *Laser Phys.*, **19**(4):836-854. [doi:10.1134/S1054660X09040434]

Timashev, S.F., Polyakov, Y.S., Misurkin, P.I., *et al.*, 2010. Anomalous diffusion as a stochastic component in the dynamics of complex processes. *Phys. Rev. E*, **81**:041128.1-041128.17. [doi:10.1103/PhysRevE.81.041128]

Timashev, S.F., Panischev, O.Y., Polyakov, Y.S., *et al.*, 2012. Analysis of cross-correlations in electroencephalogram signals as an approach to proactive diagnosis of schizophrenia. *Phys. A*, **391**(4):1179-1194. [doi:10.1016/j.physa.2011.09.032]

Watters, P.A., 1998. Fractal Structure in the Electroencephalogram. Available from http://www.complexity.org.au/ci/vol05/watters/watters.html

Wornell, G.W., 1991. Synthesis, Analysis, and Processing of Fractal Signals. PhD Thesis, Massachusetts Institute of Technology, Massachusetts, USA.

Wornell, G.W., 1993. Wavelet-based representations for the $1/f$ family of fractal processes. *Proc. IEEE*, **81**(10):1428-1450. [doi:10.1109/5.241506]

Wornell, G.W., 1995. Signal Processing with Fractals: a Wavelet-Based Approach. Prentice Hall, New Jersey, USA.

Wornell, G.W., Oppenheim, A.V., 1992. Estimation of fractal signals from noisy measurements using wavelets. *IEEE Trans. Signal Process.*, **40**(3):611-623. [doi:10.1109/78.120804]